Journal of Dental Sciences

Volume 21 | Issue 2 Article 50

2026

Quantitative comparison of enamel–dentin and dentin–pulp distances between cone-beam computed tomography and histological sections: An ex vivo study

Chi-Yu Lin

Che-Ming Liu

Yu-Chieh Lin

Sheng-Yang Lee

Wei-Chun Lin

Available online at https://jds.ads.org.tw/journal/

Digital Commons

journal homepage: https://jds.ads.org.tw/journal/

Original Article

Quantitative comparison of enamel–dentin and dentin–pulp distances between cone-beam computed tomography and histological sections: An ex vivo study

Chi-Yu Lin [a], Che-Ming Liu [b,c], Yu-Chieh Lin [d,e], Sheng-Yang Lee [b,c], Wei-Chun Lin [a,c*]

[a] *School of Dental Technology, College of Oral Medicine, Taipei Medical University, Taipei, Taiwan*
[b] *School of Dentistry, College of Oral Medicine, Taipei Medical University, Taipei, Taiwan*
[c] *Department of Dentistry, Wan Fang Hospital, Taipei Medical University, Taipei, Taiwan*
[d] *Digital Medicine Center, Translational Health Research Institute, Vilnius University, Vilnius, Lithuania*
[e] *Institute of Research, Development and Innovation, IMU University, Kuala Lumpur, Malaysia*

Received 20 November 2025; Final revision received 11 December 2025
Available online 1 April 2026

KEYWORDS
Cone-beam computed tomography;
Histology;
Enamel–dentin junction;
Dentin–pulp distance;
Measurement accuracy;
Dental imaging

Abstract *Background/purpose:* Cone-beam computed tomography (CBCT) has become an essential imaging tool in dentistry for evaluating internal tooth morphology. However, its quantitative accuracy in representing true enamel–dentin (E–D) and dentin–pulp (D–P) distances remains uncertain. This study aimed to compare CBCT-derived measurements with histological references and to assess depth-dependent discrepancies across tooth sections.
Materials and methods: A total of 18 extracted human teeth were sectioned bucco–lingually and analyzed using both CBCT and histological microscopy. For each tooth, three representative slices were selected: the first and last slices containing pulp tissue, and one at the midpoint. E–D and D–P distances were measured digitally and compared between modalities using paired *t*-tests, correlation analysis, and Bland–Altman plots.
Results: CBCT consistently overestimated E–D distances compared with histology, particularly near the pulp chamber, whereas D–P differences showed greater variability. Weak to moderate linear correlations were observed between modalities (E–D: $r = 0.45$; D–P: $r = 0.34$). Bland–Altman analysis indicated a mean bias of $+0.26$ mm for E–D and -0.09 mm for D–P, suggesting a trend toward systematic overestimation in enamel-dentin regions and inconsistent deviation patterns in deeper dentin–pulp zones.

* Corresponding author. School of Dental Technology, College of Oral Medicine, Taipei Medical University, No. 250, Wu-Xing Street, Taipei, 11031, Taiwan.
E-mail address: weichun1253@tmu.edu.tw (W.-C. Lin).

https://doi.org/10.1016/j.jds.2025.12.015

Conclusion: While CBCT provides clinically acceptable accuracy in quantifying intra-tooth structures, it tends to overestimate enamel—dentin thickness in deeper regions. These findings underline the need for refined imaging calibration to enhance quantitative reliability in endodontic and restorative applications.

Introduction

Traditional intraoral and panoramic X-rays have long served as foundational diagnostic tools in dentistry but remain constrained by two-dimensional projection, anatomical superimposition, and image distortion.[1–3] These inherent limitations prevent accurate characterization of the three-dimensional morphology of teeth and restrict the ability to visualize subtle internal changes within enamel, dentin, and pulp. As a result, diagnostic interpretation frequently depends on indirect inference rather than direct anatomical depiction, which may obscure early pathological alterations, complex anatomical configurations, or variations in mineralization. In challenging scenarios—such as assessing multi-rooted canal systems, identifying periapical pathology, evaluating resorptive defects, or planning implant placement—the lack of spatial fidelity compromises clinical precision and increases diagnostic uncertainty. Consequently, more advanced three-dimensional imaging modalities, most notably cone-beam computed tomography (CBCT), have emerged to overcome these limitations and provide enhanced diagnostic accuracy.

CBCT has become an indispensable tool in contemporary dental practice, offering volumetric visualization of internal tooth structures with substantially lower radiation exposure than conventional computed tomography. Its ability to depict enamel—dentin (E—D) and dentin—pulp (D—P) distances—parameters critical for estimating residual dentin thickness, minimizing pulp chamber perforation risk, and guiding minimally invasive restorative or endodontic procedures—has expanded its utility in clinical decision-making.[4,5] Despite widespread use, the quantitative fidelity of CBCT in replicating true tissue boundaries remains a point of concern. Unlike external bone measurements, accurately defining internal tooth interfaces presents unique challenges. Voxel-related limitations, beam hardening, scatter, and partial volume effects can introduce systematic dimensional deviations. Specifically, the "blooming" artifact caused by high-density enamel can obscure the underlying dentin boundary, while noise and reduced contrast at the dentin-pulp interface can mask the true pulp chamber walls.[6,7] These issues become even more pronounced when anatomical complexity increases or when clinicians rely on submillimeter accuracy for treatment planning.

Histological analysis serves as the gold standard for resolving internal tooth morphology, providing direct, high-resolution measurement of structural interfaces. Comparative ex vivo studies evaluating CBCT against micro-CT or histology generally demonstrate good accuracy in enamel and coronal dentin, yet consistently report decreasing precision in deeper or low-density regions.[8,9] Such discrepancies may reflect both the intrinsic complexity of dental anatomy and the technical constraints of CBCT imaging. Accordingly, quantitative assessment using regression, Bland—Altman analysis, and related statistical methods has become essential for determining measurement reliability and detecting systematic biases between modalities.[10] These analytical frameworks also allow researchers to explore depth-dependent variability, helping to identify where CBCT performance begins to diverge from histological truth.

Given these anatomical and technical considerations, the present study aimed to quantitatively compare E—D and D—P distances from CBCT and histological sections across different tooth depths, highlighting how measurement discrepancies vary with depth, tissue density, and CBCT imaging performance. We hypothesized that CBCT measurement accuracy is depth-dependent, with greater dimensional deviation expected at the dentin-pulp interface compared to the enamel-dentin junction due to beam hardening and reduced contrast resolution in deeper tooth regions.

Materials and methods

This study was approved by the Institutional Review Board of Taipei Medical University—Wanfang Hospital (TMU-JRB No.: N202504065). The overall experimental workflow is illustrated in Fig. 1. A total of 21 extracted human teeth without visible caries, fractures, or restorations were initially collected from patients requiring orthodontic treatment. After macroscopic evaluation, three teeth were excluded due to incomplete crown or root morphology, resulting in 18 teeth for analysis (comprising 8 premolars and 10 M). Posterior teeth were specifically selected for this study due to their complex internal anatomy and greater crown volume compared to anterior teeth. This selection allowed for multiple distinct cross-sectional slices per specimen to evaluate depth-dependent measurement variability. Furthermore, the thicker enamel and dentin in posterior teeth present a more challenging scenario for CBCT imaging due to increased beam hardening and scattering, serving as a rigorous model for assessing quantitative limitations. Each tooth was embedded in resin and serially sectioned to a thickness of approximately 1 mm in the bucco—lingual direction using a precision diamond saw (CL40, TOPTECH, Taichung, Taiwan) under continuous

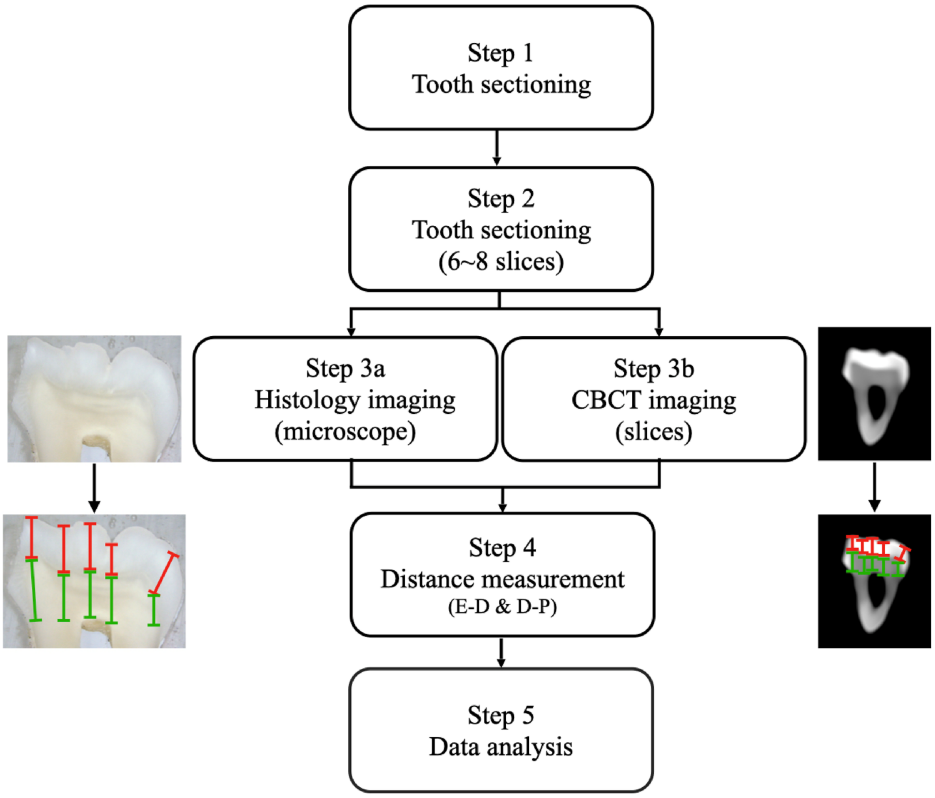

Figure 1 Workflow of the experimental procedure. Schematic illustration of the methodological workflow. Extracted teeth were sectioned into slices, followed by histological and CBCT imaging. Measurements of enamel–dentin (E–D) and dentin–pulp (D–P) distances were obtained and analyzed to compare morphological differences and assess agreement between modalities. CBCT: Cone-beam computed tomography.

water cooling to prevent thermal damage and maintain dimensional integrity. On average, six slices were obtained per tooth, resulting in a total of 108 slices from the 18 specimens. From these, three representative slices were selected for measurement: (1) the first slice where the pulp chamber first appeared, (2) the last slice where pulp was still visible, and (3) the central slice between these two. These three slices served as the final specimens for histological and CBCT comparison.

Each selected slice was examined using an optical microscope (Leica Microsystems, Wetzlar, Germany) under calibrated magnification. High-resolution digital images were captured, and linear distances between enamel–dentin (E–D) and dentin–pulp (D–P) interfaces were measured using LAS X software (Leica Microsystems, Wetzlar, Germany). Each measurement was repeated three times by two independent observers in order to ensure reproducibility.

All slices were scanned individually using a cone-beam computed tomography (CBCT, ProMax 3D Plus, Planmeca, Finland). The acquired DICOM data were reconstructed with Romexis Viewer software (version 5.3, PLANMECA OY, Helsinki, Finland). To ensure spatial consistency between the two modalities, a rigorous alignment protocol was implemented. First, the CBCT volume was reoriented using Multi-Planar Reconstruction (MPR) to align the viewing plane parallel to the physical bucco-lingual sectioning axis. Subsequently, the specific CBCT slice corresponding to each histological section was identified using landmark-based visual registration.

Matching was confirmed by aligning three key anatomical reference markers: (1) the specific morphology of the pulp chamber and pulp horns, (2) the cross-sectional profile of the cemento-enamel junction (CEJ), and (3) the crown contour. Once the corresponding slices were identified, the linear distances for E–D and D–P measurements were defined following the methodology described in our previous study.[11] Specifically, measurements were taken perpendicular to the tangent of the tissue interface to ensure geometric validity.

For both CBCT and histology, five measurement points were selected within each region of interest. The mean values and standard deviations (SD) of E–D and D–P distances were calculated per slice and per tooth. The mean difference between modalities (CBCT minus Histology) was computed for each slice to evaluate systematic bias. Positive differences indicated overestimation by CBCT, whereas negative differences reflected underestimation relative to histological measurements.

Measurement data were analyzed using IBM SPSS Statistics (version 31.0, IBM Corp., Armonk, NY, USA) and SigmaPlot (version 16, San Jose, CA, USA). To preserve the resolution of depth-related variations, the statistical unit of analysis was defined at the slice level ($n = 54$, derived from 3 representative slices across 18 teeth). Intra-observer and inter-observer reliability were assessed using

the Intraclass Correlation Coefficient (ICC). Paired t-tests were used to compare CBCT and histological data for both E—D and D—P measurements, with statistical significance set at $P < 0.05$. Differences and variability were visualized using box plots and heatmaps, while correlation and agreement between modalities were assessed using scatter plots and Bland—Altman plots to evaluate measurement fidelity and potential systematic bias.

Results

Excellent reliability was demonstrated for all measurements. The intra-observer ICCs ranged from 0.955 to 0.964, and inter-observer ICCs ranged from 0.981 to 0.990. The mean and standard deviation of E—D and D—P measurements obtained from CBCT and histological sections are summarized in Tables 1 and 2. CBCT-derived E—D distances were generally greater than those measured histologically, whereas D—P values showed greater variability. Fig. 2 illustrates these differences across teeth, revealing a mild overestimation of E—D distances by CBCT and mixed patterns of over- and underestimation for D—P. The dispersion of D—P data suggests that measurement reliability decreases with increasing structural depth, likely due to attenuation loss and reduced grayscale contrast near the pulp. Although CBCT captures consistent geometric morphology, voxel resolution and reconstruction fidelity continue to influence quantitative accuracy.

To evaluate intra-tooth variability, slice-based mean differences between CBCT and histological measurements were analyzed (Tables 3 and 4). The mean differences (CBCT − Histology) ranged from −0.54 mm to +1.07 mm for E—D and −2.14 mm to +1.60 mm for D—P, indicating depth-dependent bias. The heatmap in Fig. 3 illustrates the measurement differences (CBCT − Histology) for E—D (A) and D—P (B) distances. Red tones represent CBCT overestimation, whereas blue tones indicate underestimation. E—D regions show a predominantly positive bias, while D—P regions display greater variability, highlighting depth-dependent and region-specific discrepancies in CBCT measurement accuracy. These findings indicate that discrepancies were most evident in teeth with thinner enamel or larger pulp chambers, emphasizing the role of morphological complexity in CBCT measurement accuracy.

Statistical comparison between modalities (Tables 5 and 6) revealed correlations between CBCT and histological measurements, yet several teeth showed significant deviations—particularly for E—D distances. The observation that these significant differences appeared in specific teeth, rather than randomly across the sample, points to systematic measurement errors driven by local anatomy rather than random variation. Specifically, CBCT consistently overestimated enamel—dentin thickness, reflecting systematic blooming artifacts typical of high-density structures, whereas D—P depth displayed variable accuracy with mixed over- and underestimation due to lower contrast at the soft-tissue interface. These results indicate that structural complexity, such as enamel curvature and pulp chamber morphology, can induce systematic errors in CBCT-derived measurements. Consequently, the presence of significant bias in specific teeth suggests that localized anatomy may amplify reconstruction artifacts or beam

Table 1 Comparison of enamel—dentin (E—D) distance measurements (mm) between CBCT and histological sections for each tooth.

Tooth number	CBCT		Histology	
	Mean	SD	Mean	SD
1	2.01	0.30	1.97	0.54
2	2.03	0.20	2.04	0.22
3	1.87	0.12	1.98	0.19
4	2.04	0.24	2.10	0.43
5	2.20	0.36	2.02	0.56
6	1.70	0.17	1.33	0.18
7	2.26	0.11	1.59	0.53
8	1.87	0.12	1.66	0.37
9	2.56	0.15	2.06	0.19
10	1.96	0.08	1.48	0.31
11	2.43	0.13	1.89	0.50
12	2.54	0.25	1.96	0.18
13	2.46	0.12	2.11	0.25
14	2.29	0.30	2.26	0.33
15	2.48	0.28	2.14	0.31
16	2.17	0.07	2.01	0.46
17	2.16	0.33	1.83	0.35
18	2.39	0.37	2.24	0.13

CBCT: Cone-beam computed tomography.
SD: Standard deviation.

Table 2 Comparison of dentin-pulp (D-P) distance measurements (mm) between CBCT and histological sections for each tooth.

Tooth number	CBCT		Histology	
	Mean	SD	Mean	SD
1	3.28	0.66	2.93	0.59
2	2.63	0.32	2.78	0.45
3	3.39	0.13	3.08	0.94
4	2.90	0.57	3.28	0.52
5	3.47	0.74	3.54	0.34
6	2.83	0.20	2.65	0.34
7	3.00	0.18	3.08	0.25
8	3.22	0.43	3.18	0.37
9	2.98	0.19	3.14	0.29
10	3.23	0.29	3.07	0.74
11	2.59	0.19	4.13	0.63
12	3.60	0.13	3.01	0.45
13	3.63	0.72	4.00	0.35
14	2.25	0.68	2.31	0.63
15	3.43	0.33	3.16	0.49
16	3.25	0.35	3.70	0.53
17	3.13	0.15	3.21	0.39
18	3.25	0.12	3.34	0.48

CBCT: Cone-beam computed tomography.
SD: Standard deviation.

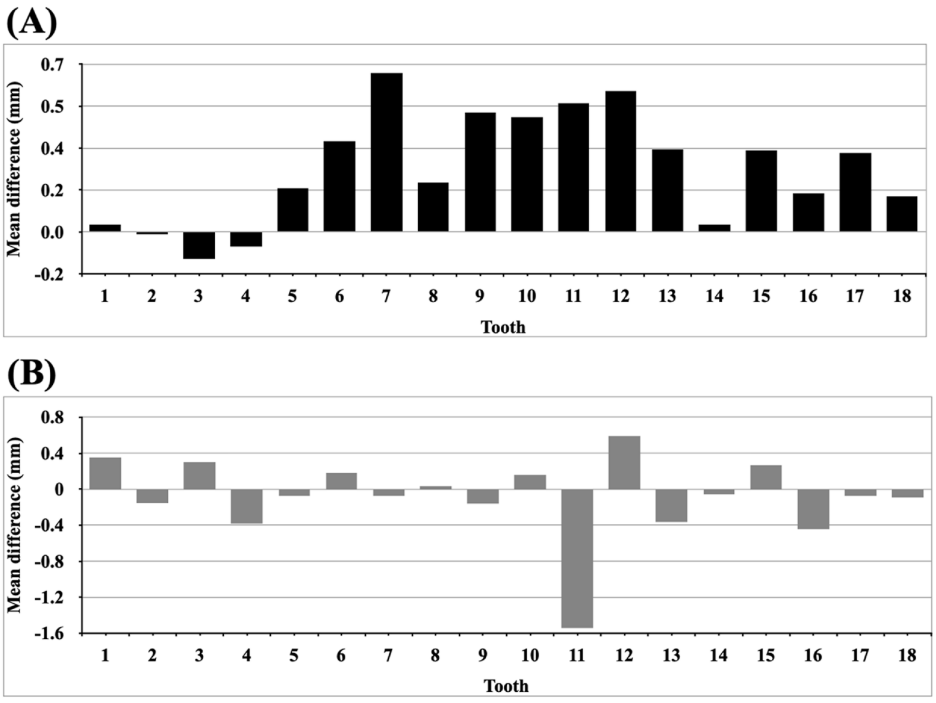

Figure 2 Mean differences between CBCT and histological measurements for individual teeth. Comparison of mean differences (CBCT − Histology, mm) in E–D (A) and D–P (B) distances across 18 teeth. Each bar represents the averaged measurement difference per tooth. CBCT: Cone-beam computed tomography.

Table 3 Mean differences (mm) in enamel–dentin (E–D) measurements for each slice of individual teeth.

Tooth number	Mean difference (CBCT-histology)		
	Slice 1	Slice 2	Slice 3
1	−0.23	−0.23	−0.23
2	0.28	−0.20	−0.11
3	0.15	−0.28	−0.21
4	−0.05	−0.54	0.40
5	0.03	0.11	0.41
6	0.39	0.40	0.35
7	−0.03	1.02	1.01
8	0.22	0.68	−0.29
9	0.56	0.81	0.13
10	0.13	0.66	0.65
11	0.87	0.80	−0.07
12	0.26	0.44	1.07
13	0.24	0.18	0.61
14	−0.28	0.25	0.12
15	0.16	0.48	0.39
16	−0.39	0.66	0.21
17	0.11	0.25	0.63
18	0.44	−0.16	0.16

CBCT: Cone-beam computed tomography.
Mean difference values (mm), calculated as CBCT minus histological measurements, across three slices (Slice 1–3) for each tooth.

Table 4 Mean differences (mm) in dentin-pulp (D-P) measurements for each slice of individual teeth.

Tooth number	Mean difference (CBCT-histology)		
	Slice 1	Slice 2	Slice 3
1	1.60	−0.18	−0.37
2	0.06	−0.44	−0.08
3	1.31	−0.60	0.21
4	−1.14	−0.30	0.30
5	1.01	−0.86	−0.38
6	0.21	0.33	0.01
7	−0.01	−0.15	−0.07
8	−0.15	−0.14	0.40
9	−0.11	−0.30	−0.08
10	0.63	−0.33	0.18
11	−1.35	−1.15	−2.14
12	0.10	0.53	1.14
13	−0.94	−0.27	0.11
14	0.19	−0.28	−0.10
15	0.25	0.00	0.55
16	0.01	−0.54	−0.80
17	0.48	−0.31	−0.39
18	0.22	0.28	−0.77

CBCT: Cone-beam computed tomography.
Mean difference values (mm), calculated as CBCT minus histological measurements, across three slices (Slice 1–3) for each tooth.

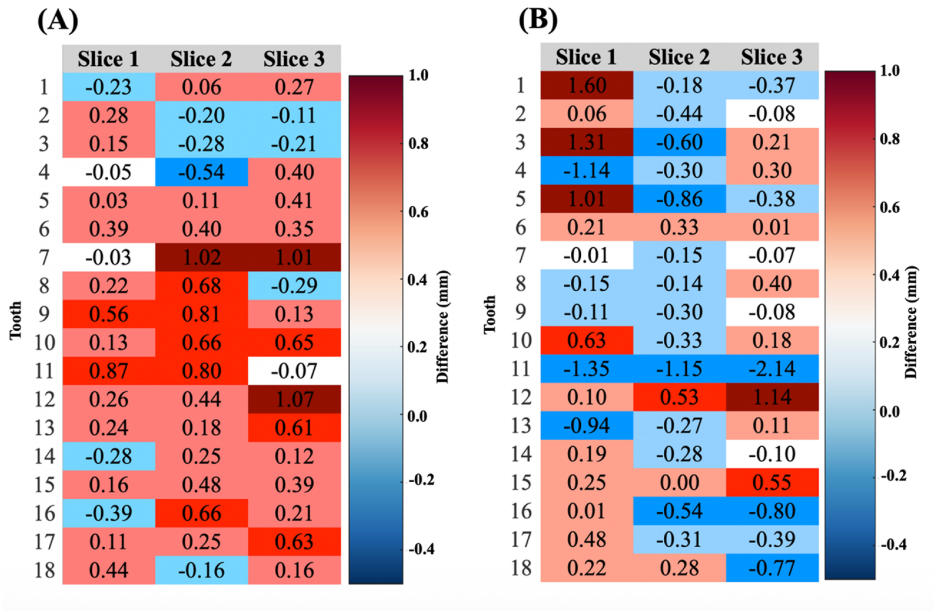

Figure 3 Heatmap visualization of measurement differences. Heatmaps displaying the slice-wise differences between CBCT and histological measurements (CBCT − Histology, mm) for enamel—dentin (E—D) distances (A) and dentin—pulp (D—P) distances (B) across all teeth. Warmer colors (red tones) represent greater positive differences, indicating that CBCT yielded larger values than histology (overestimation). Cooler colors (blue tones) represent negative differences, indicating that CBCT produced smaller values than histology (underestimation). These patterns highlight spatial variability both within individual teeth and among specimens, reflecting depth- and region-dependent measurement discrepancies. CBCT: Cone-beam computed tomography.

Table 5 Statistical comparison of enamel—dentin (E—D) measurements between CBCT and histological sections for each tooth.

Tooth number	Mean		Mean difference	*P* value
	CBCT	Histology		
1	2.01	1.97	0.03	0.75
2	2.03	2.04	−0.01	0.96
3	1.87	1.98	−0.11	0.48
4	2.04	2.10	−0.06	0.75
5	2.20	2.02	0.18	0.25
6	1.70	1.33	0.38	**0.001****
7	2.26	1.59	0.66	0.20
8	1.87	1.66	0.20	0.54
9	2.56	2.06	0.50	0.13
10	1.96	1.48	0.48	0.11
11	2.43	1.89	0.54	0.22
12	2.54	1.96	0.59	0.14
13	2.46	2.11	0.34	0.12
14	2.29	2.26	0.03	0.86
15	2.48	2.14	0.34	0.07
16	2.17	2.01	0.16	0.65
17	2.16	1.83	0.33	0.17
18	2.39	2.24	0.15	0.48

CBCT: Cone-beam computed tomography.
Mean (mm) values obtained from CBCT and histological measurements for each tooth, together with the calculated mean difference (CBCT minus histology) and corresponding *P* values derived from paired *t* tests. **P = Indicated significant difference ($P < 0.01$).

Table 6 Statistical comparison of dentin-pulp (D-P) measurements between CBCT and histological sections for each tooth.

Tooth number	Mean		Mean difference	*P* value
	CBCT	Histology		
1	3.28	2.93	0.35	0.632
2	2.63	2.78	−0.16	0.406
3	3.39	3.08	0.31	0.636
4	2.90	3.28	−0.38	0.459
5	3.47	3.54	−0.08	0.905
6	2.83	2.65	0.18	0.188
7	3.00	3.08	−0.07	0.212
8	3.22	3.18	0.04	0.853
9	2.98	3.14	−0.16	0.141
10	3.23	3.07	0.16	0.630
11	2.59	4.13	−1.54	**0.036***
12	3.60	3.01	0.59	0.190
13	3.63	4.00	−0.37	0.350
14	2.25	2.31	−0.06	0.707
15	3.43	3.16	0.27	0.230
16	3.25	3.70	−0.45	0.201
17	3.13	3.21	−0.07	0.817
18	3.25	3.34	−0.09	0.811

CBCT: Cone-beam computed tomography.
Mean (mm) values obtained from CBCT and histological measurements for each tooth, together with the calculated mean difference (CBCT minus histology) and corresponding *P* values derived from paired *t* tests. *P = Indicated significant difference ($P < 0.05$).

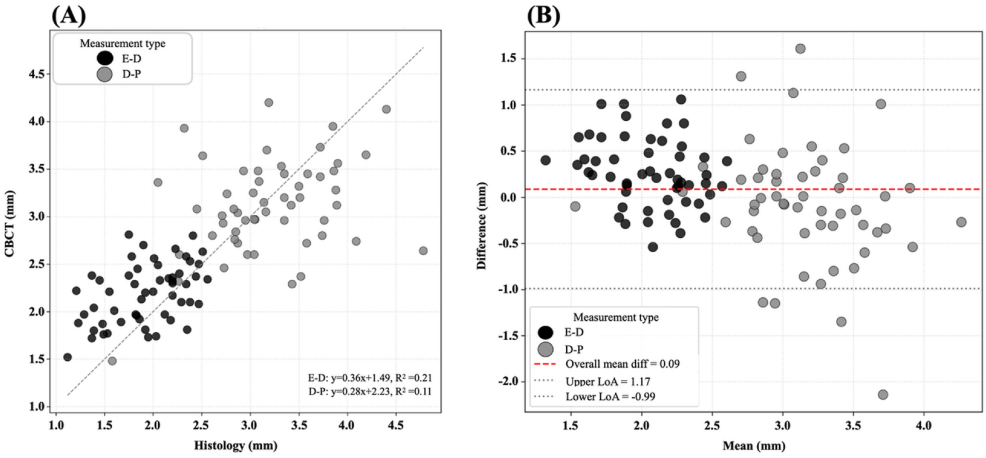

Figure 4 Correlation and agreement between CBCT and histological measurements. (A) Scatter plot illustrated the correlation between CBCT and histological measurements for E–D (black) and D–P (gray). Regression lines and corresponding equations with R^2 values are displayed within the plot (E–D: $y = 0.36x + 1.49$, $R^2 = 0.21$; D–P: $y = 0.28x + 2.23$, $R^2 = 0.11$). Correlation analysis demonstrated weak to moderate associations between modalities (E–D: $r = 0.45$; D–P: $r = 0.34$). (B) Bland–Altman plot illustrating measurement agreement. Black and gray dots correspond to E–D and D–P, respectively. The red dashed line indicates the mean bias, and gray dotted lines denote the 95 % limits of agreement (LoA), calculated as the mean difference ±1.96 standard deviations of the differences. CBCT: Cone-beam computed tomography.

hardening, especially in regions with sharp curvature or heterogeneous density.

As shown in the correlation and agreement analysis (Fig. 4A and B), both modalities exhibited weak to moderate relationships between CBCT and histological measurement for enamel–dentin (E–D) and dentin–pulp (D–P) distances. Based on the slice-level analysis ($n = 54$) (Fig. 4A), E–D measurements demonstrated a correlation coefficient of $r = 0.45$ with a corresponding $R^2 = 0.21$, indicating that CBCT explained approximately 21 % of the variance observed in histology. D–P measurements exhibited even lower consistency ($r = 0.34$, $R^2 = 0.11$), suggesting limited predictive agreement across modalities. Although a positive linear trend was present in both datasets, the wide dispersion of data points—particularly within deeper dentin and pulp regions—highlights substantial variability in CBCT-derived values. In addition, Bland–Altman analysis (Fig. 4B) revealed a measurable bias, with CBCT readings consistently exceeding histological values by approximately 0.26 mm. Although most data points fell within the 95 % limits of agreement (LoA), defines as the mean difference ±1.96 standard deviations, the observed systematic overestimation reflects intrinsic limitations of CBCT imaging rather than random variability. The bias likely arises from voxel interpolation, grayscale averaging, and partial volume effects that obscure true tissue interfaces and inflate dimensional measurements. Consequently, CBCT does not faithfully reproduce histological spatial accuracy and may misrepresent fine anatomical boundaries—particularly in thin enamel or near the pulp chamber. These findings indicate that CBCT-derived distances should be interpreted as approximate rather than absolute morphometric representations, reinforcing the need for careful calibration and multimodal validation when applied to quantitative dental analysis.

Discussion

This study quantitatively compared enamel–dentin (E–D) and dentin–pulp (D–P) distances between CBCT and histological sections. Our results revealed a distinct dichotomy in measurement accuracy: CBCT measurements tended to overestimate E–D thickness—specifically showing a systematic mean bias of +0.26 mm in our Bland–Altman analysis—while exhibiting greater variability in D–P depths. These findings align with previous studies reporting that CBCT often yields larger dimensional values than histological or micro-CT analyses due to voxel interpolation and limited spatial resolution at tissue boundaries.[12,13] However, the specific magnitude of this overestimation observed in our data can be directly attributed to the "blooming artifact" alongside partial volume effects. Because enamel possesses extremely high radiopacity, the signal tends to bleed into adjacent voxels during reconstruction. This effect blurs the sharp histological E–D boundary, causing the high-density enamel to appear thicker on CBCT than in reality. When enamel thickness approaches voxel size, boundaries become ambiguous, producing the apparent dimensional enlargement we observed across the majority of slice samples (Fig. 3A). Additionally, minor fluctuations in grayscale intensity and reconstruction noise can further distort the perceived location of tissue transitions, particularly in regions with steep density gradients. These factors collectively contribute to the systematic positive bias in CBCT-derived measurements and underscore the challenges of achieving histology-level precision with current clinical imaging systems.

In contrast to the systematic bias seen in enamel, variations in D–P measurements were characterized by random variability and lower predictive reliability ($R^2 = 0.11$). This

finding indicates that soft-tissue regions, such as the pulp, are more susceptible to contrast loss and beam-hardening artifacts. Similar observations have shown that low-density areas in CBCT reconstructions often display signal attenuation and nonuniform grayscale distribution near pulp horns or curved internal structures.[14] Such instability in grayscale fidelity explains why our heatmap (Fig. 3B) displayed mixed patterns of over- and underestimation, as the software struggled to consistently define the dentin—pulp boundary. These results suggest that CBCT measurement fidelity depends on both tissue depth and density—performing with consistent bias in enamel but less predictably in deeper dentin and pulp regions. This characteristic is particularly relevant to minimally invasive and endodontic treatment planning, where even small deviations in remaining dentin thickness or pulp proximity may influence access design, risk assessment, and procedural safety.

A key factor behind this bias is CBCT's limited contrast resolution and boundary sharpness. For instance, Tanaka et al. reported that buccal bone thickness was overestimated by approximately 0.12 mm when the actual thickness was below 2 mm.[15] Other studies have demonstrated that voxel size, beam hardening, and partial volume artifacts significantly affect CBCT accuracy.[16–18] Our previous study also noted that indistinct transitions between the enamel—dentin and dentin—pulp interfaces in CBCT slices hinder the clear delineation of internal tooth structures.[11] Computational studies further confirmed that reconstruction errors increase with depth and reduced contrast in low-density regions, leading to progressive distortion of anatomical boundaries.[19,20] Moreover, imaging parameters such as cone-beam geometry, scattered radiation, and reconstruction kernel selection can compound boundary uncertainty, especially in small, thin, or highly curved features where grayscale gradients become shallow. Although smaller voxels or advanced reconstruction filters may mitigate some of these limitations, they often introduce compromise such as increased noise, longer scan times, or higher radiation dosage. Collectively, these findings emphasize that CBCT resolution and artifact behavior are closely tied to tissue density and morphology, ultimately dictating its quantitative precision in endodontic and restorative applications.

Although weak to moderate liner correlations between CBCT and histology (E—D: $r = 0.45$; D—P: $r = 0.34$), several teeth demonstrated notable deviations, particularly in E—D measurements. This suggests that although CBCT provides clinically useful morphological estimates, it cannot fully replicate the dimensional precision achieved by histological evaluation, especially within deeper dentin and pulp regions where contrast gradients diminish. Such discrepancies may arise from anatomical variability— including differences in enamel curvature, secondary dentin deposition, pulp chamber morphology, or age-related changes in mineral density—all of which influence X-ray attenuation and boundary clarity.[20] Methodological limitations should also be considered, including the relatively small sample size, ex vivo conditions lacking in vivo motion and soft-tissue context, potential micro-distortion during sectioning, and reliance on a single CBCT device and acquisition protocol. These factors may restrict generalizability. Future investigations employing larger cohorts that includes anterior teeth, multiple imaging systems, and AI-driven artifact reduction algorithms are essential to verify these findings across the entire dentition and improve cross-modality reproducibility.

Nevertheless, it is crucial to contextualize these discrepancies within clinical standards. Previous studies on CBCT linear measurement accuracy and endodontic working length determination typically regard a deviation of less than 0.5 mm as the threshold for clinical acceptability.[21,22] In this study, the mean systematic bias for E-D distance was $+0.26$ mm, and the majority of D-P deviations fell within the 95 % limits of agreement of approximately ± 1.0 mm (Fig. 4B). While the E-D bias is well within the 0.5 mm tolerance—suggesting that CBCT is reliable for assessing enamel thickness and crown preparations—the higher variability in D-P measurements warrants caution.

This study extends the current understanding of CBCT by shifting focus from general accuracy to the specific impact of depth on imaging artifacts. Unlike earlier research that largely concentrated on external dimensions or overall averages,[8,15,23] our work demonstrates that measurement error is not uniform throughout the tooth; instead, it varies by structure. We observed a clear distinction in error patterns: high-contrast enamel boundaries tend to be systematically overestimated due to blooming, while low-contrast pulp interfaces in deeper regions are subject to random variability caused by signal attenuation. Clinically, this implies that a single 'safety margin' is insufficient for all internal measurements. While submillimeter precision appears reliable for coronal preparations, clinicians should apply larger tolerance zones when working in deep pulp spaces, where beam hardening obscures the true anatomy more than previously understood.

In summary, CBCT remains a valuable modality for three-dimensional visualization of internal tooth anatomy and generally provides clinically acceptable measurement reliability. However, its susceptibility to systematic overestimation and depth-dependent variability—particularly when compared with histological standards—underscores the need for cautious interpretation. Submillimeter discrepancies near the pulp chamber may meaningfully influence decisions in minimally invasive preparations or endodontic access, making clinicians' awareness of CBCT artifacts indispensable. Accurate assessment therefore requires considering CBCT findings with both clinical judgment and histological knowledge. Looking ahead, the integration of AI-driven enhancement, real-time artifact suppression technologies, and multimodal validation frameworks holds promise for improving quantitative fidelity. Such advances may narrow the gap between radiographic and histological precision, ultimately enabling safer, more predictable, and data-driven dental interventions.

Declaration of competing interest

The authors have no conflicts of interest relevant to this article.

Acknowledgments

This research is financially supported by the National Science and Technology Council of Taiwan (NSTC 114-2314-B-038-051) to Wei-Chun Lin.

References

1. Danjo A, Kuwada C, Aijima R, et al. Limitations of panoramic radiographs in predicting mandibular wisdom tooth extraction and the potential of deep learning models to overcome them. *Sci Rep* 2024;14:30806.
2. Turosz N, Checinska K, Checinski M, Sielski M, Sikora M. Evaluation of dental panoramic radiographs by artificial intelligence compared to human reference: a diagnostic accuracy study. *J Clin Med* 2024;13:6859.
3. Lingam AS, Koppolu P, Abdulsalam R, Reddy RL, Anwarullah A, Koppolu D. Assessment of common errors and subjective quality of digital panoramic radiographs in dental institution, Riyadh. *Ann Afr Med* 2023;22:49–54.
4. Llacer-Martinez M, Martin-Biedma B, Sanz MT, et al. Cone-beam computed tomography for the evaluation of dental pulp chamber volume: implications for clinics and teaching. *Dent J (Basel)* 2024;12:95.
5. Wei X, Du Y, Zhou X, et al. Expert consensus on digital guided therapy for endodontic diseases. *Int J Oral Sci* 2023;15:54.
6. Wajer R, Dabrowski-Tumanski P, Wajer A, Kazimierczak N, Serafin Z, Kazimierczak W. Enhancing image quality in dental-maxillofacial CBCT: the impact of iterative reconstruction and ai on noise reduction-A systematic review. *J Clin Med* 2025;14:4214.
7. Razumova S, Brago A, Barakat H, et al. Evaluation of dentinal thickness and remaining dentine volume around root canals using cone-beam computed tomography scanning. *Dent J (Basel)* 2023;11:124.
8. Choudhari S, Venkata Teja K, Ramesh S, et al. Assessment of anatomical dentin thickness in mandibular first molar: an in vivo cone-beam computed tomographic study. *Int J Dent* 2024;2024:8823070.
9. Yazdizadeh M, Alavinezhad P, Sadrishahrezaei A, Sharifishoshtari S. Root canal morphology of mandibular first molars: comparison of the diagnostic accuracy of cone-beam computed tomography and the sectioning technique. *Dent Res J (Isfahan)* 2023;20:103.
10. Bose MWH, Buchholz J, Beuer F, Pieralli S, Bumann A. Evaluation of ultra-low-dose CBCT protocols to investigate vestibular bone defects in the context of immediate implant planning: an ex vivo study on cadaver skulls. *J Clin Med* 2025;14:4196.
11. Lin YC, Cheng FC, Lin WC, Chiang CP. Artificial intelligence measurement of multi-layer tooth structures using semantic segmentation and computer vision. *J Dent Sci* 2025;20:723–5.
12. Henaut M, Meire M, Vandomme J, Robberecht L. Evaluation of cone beam computed tomography resolution, 3D printing resolution and drilling depth on drilling accuracy in guided endodontics: an in-vitro study. *Eur Endod J* 2025;10:127–33.
13. Acar B, Kamburoglu K, Tatar I, et al. Comparison of micro-computerized tomography and cone-beam computerized tomography in the detection of accessory canals in primary molars. *Imaging Sci Dent* 2015;45:205–11.
14. Wagendorf O, Nahles S, Vach K, et al. The impact of teeth and dental restorations on gray value distribution in cone-beam computer tomography: a pilot study. *Int. J. Implant Dent.* 2023;9:27.
15. Tanaka Y, Dutra V, Lin WS, Levon J, Hamada Y. Evaluation of the accuracy of buccal bone thickness measurement from cone beam computed tomography compared with histologic analysis. *J Prosthet Dent* 2023;130:68–73.
16. Tayman MA, Kamburoglu K, Ocak M, Ozen D. Effect of different voxel sizes on the accuracy of CBCT measurements of trabecular bone microstructure: a comparative micro-CT study. *Imaging Sci Dent* 2022;52:171–9.
17. Lennholm C, Andreasen H, Westerlund A, Lund H. Visibility of alveolar bone thicknesses on CBCT images-a study on minimum bone requirements using various reconstruction techniques, viewing modes, and resolutions. *Clin Oral Invest* 2024;28:641.
18. Terrabuio BR, Carvalho CG, Peralta-Mamani M, Santos P, Rubira-Bullen IRF, Rubira CMF. Cone-beam computed tomography artifacts in the presence of dental implants and associated factors: an integrative review. *Imaging Sci Dent* 2021;51:93–106.
19. Park HSHC, Seo JK. Nonlinear ill-posed problem in low-dose dental cone-beam computed tomography. *IMA J Appl Math* 2024;89:231–53.
20. Kaasalainen T, Ekholm M, Siiskonen T, Kortesniemi M. Dental cone beam CT: an updated review. *Phys Med* 2021;88:193–217.
21. Nikneshan S, Aval SH, Bakhshalian N, Shahab S, Mohammadpour M, Sarikhani S. Accuracy of linear measurement using cone-beam computed tomography at different reconstruction angles. *Imaging Sci Dent* 2014;44:257–62.
22. Sherrard JF, Rossouw PE, Benson BW, Carrillo R, Buschang PH. Accuracy and reliability of tooth and root lengths measured on cone-beam computed tomographs. *Am J Orthod Dentofacial Orthop* 2010;137(4 Suppl):S100–8.
23. Yen CY, Kuo PJ, Lin CY, et al. Accuracy of cone beam computed tomography in measuring thicknesses of hard-tissue-mimicking material adjacent to different implant thread surfaces. *J Dent Sci* 2019;14:119–225.